Developmental and Comparative Immunology 34 (2010) 300–307

Contents lists available at ScienceDirect

Developmental and Comparative Immunology

journal homepage: www.elsevier.com/locate/dci

Molecular cloning and functional characterization of caspase 9 in large yellow croaker (*Pseudosciaena crocea*)

Yinnan Mu [a,1], Xiaoqiang Xiao [a,b,1], Jinzhou Zhang [a,1], Jingqun Ao [a,*], Xinhua Chen [a,*]

[a] Key Laboratory of Marine Biogenetic Resources, Third Institute of Oceanography, State Oceanic Administration, Xiamen 361005, PR China
[b] School of Life Sciences, Zhongshan University, Guangzhou 510275, PR China

ARTICLE INFO

Article history:
Received 4 October 2009
Received in revised form 26 October 2009
Accepted 26 October 2009
Available online 11 November 2009

Keywords:
Large yellow croaker (*Pseudosciaena crocea*)
Caspase 9
Site-directed mutagenesis
Proteolytic activity
Expression modulation

ABSTRACT

The genomic and cDNA sequences of a caspase 9 homologue were cloned from large yellow croaker (*Pseudosciaena crocea*). The large yellow croaker caspase 9 gene (*Lyccasp9*) consists of 10 exons and 9 introns, spanning 3836 nucleotides. The full-length cDNA of *Lyccasp9* is 2595 bp with an open reading frame of 1314 bp encoding a polypeptide of 437 amino acids (aa), which includes a 90-aa caspase recruitment domain (CARD, residues 1–90), a 133-aa p20 domain (residues 171–303) with two putative caspase family histidine and cysteine active sites, as well as an 87-aa p10 domain (residues 348–435). Recombinant Lyccasp9 (rLyccasp9) demonstrated obvious proteolytic activity. However, when histidine^{249} in the histidine active site was replaced by aspartic acid (D), or cysteine^{299} in the cysteine active site was replaced by glycine (G), the mutated rLyccasp9 (rLyccasp9-Mut-His^{249}-D or rLyccasp9-Mut-Cys^{299}-G) displayed significantly decreased proteolytic activity. Moreover, the proteolytic activity of rLyccasp9-Mut-Cys^{299}-G was lower than that of rLyccasp9-Mut-His^{249}-D, indicating that both the histidine and cysteine active sites are essential in maintaining the Lyccasp9 proteolytic activity and that the latter is more important. The *Lyccasp9* was constitutively expressed in all analyzed tissues, although expression levels varied from tissue to tissue. Real-time PCR analysis revealed that *Lyccasp9* transcript in spleen and kidney was quickly increased and then slowly decreased after stimulation with either poly(I:C), a viral mimic, or inactivated trivalent bacterial vaccine. On the other hand, enzyme activities of caspase 9 were also increased in these two tissues post-stimulation, suggesting that the activation of the intrinsic apoptotic pathway may be involved in the immune response induced by poly(I:C) or bacterial vaccine in large yellow croaker.

1. Introduction

Apoptosis is a genetically programmed cell death trigged by a variety of physiological or pathological stimuli [1,2]. It is characterized by a series of distinct morphological and biochemical changes caused by the activation of a family of intracellular cysteine aspartyl specific proteases known as caspases, which cleave many vital cellular substrates contributing to cell death and to the apoptotic phenotype. All together, 13 caspases have been identified and 11 of them were found in human [3,4]. Based on the function they performed, caspases can be categorized into inflammatory caspases (caspases 1, 4, 5 and 13) and apoptotic caspases (caspases 2, 3 and 6–10). Depending on the point they enter the apoptotic pathway, the apoptotic caspases are considered as initiator caspases (caspases 2 and 8–10) or effector caspases (caspases 3, 6 and 7) [5–7]. Generally, caspases are synthesized as inactive zymogens sharing the same domain organization containing an N-terminal prodomain ranging from 23 to 219 amino acid residues followed by a large subunit (p20 domain) and a small subunit (p10 domain)[3]. Initiator caspases usually have large prodomains containing protein-protein interaction domains, typically caspase recruitment domains (CARD, caspases 2 and 9) [8,9] or death effector domains (DEDs, caspases 8 and 10) which can recruit adaptor proteins to activate the downstream effector caspases [7]. The effector caspases commonly have a short prodomain without any apparent protein motifs [3,9].

In mammals, apoptosis can be divided into the intrinsic and extrinsic apoptotic pathways depending on how the apoptotic signal was transduced [10,11]. Human caspase 9, the pivotal initiator caspase of the intrinsic apotosis pathway, has a 130-aa prodomain mainly consisting of CARD domain, as well as a large and a small subunit. Human caspase 9 forms a multi-protein complex called apoptosome with ATP/dATP, apoptotic protease-activating factor-1 (Apaf-1) and cytochrome C released from

* Corresponding authors. Tel.: +86 592 2195297; fax: +86 592 2085376.
E-mail addresses: ajingqun2003@yahoo.com.cn (J. Ao), Chenxinh@tom.com (X. Chen).
[1] These authors contributed equally to this paper.

0145-305X/$ – see front matter © 2009 Elsevier Ltd. All rights reserved.
doi:10.1016/j.dci.2009.10.009

Table 1
Primers used in this study.

Name	Sequence	Function	Position
P1	5′-CAYTGYCTIATHATHAAYAAY-3′	cDNA fragment cloning	520–540 nt
P2	5′-YTTICGIAGRAARTTRAA-3′		1270–1287 nt
P3	5′-AGAGAGTCACTGCTGGATGACATC-3′	5′ RACE cloning	996–1019 nt
P4	5′-ACAGCATGATGACCACACAGCAGTC-3′		718–742 nt
P5	5′-AGCTCTATGTAAGATGGACCACTC-3′	3′ RACE cloning	687–710 nt
P6	5′-GATGAGGTCCAGCCATCTATC-3′		937–957 nt
P7	5′-GCCTACTGATGATCAGTCGATGG-3′	Genome DNA cloning	−214 to −192 nt
P8	5′-GACAATGACTGAACCGATT-3′		2285–2303 nt
P9	5′-AGGAATTCGTGGATAAGCGCATAAAAGAT-3′	Protein expression	358–378 nt
p10	5′-GGGTCGACCTACGCTTGGCTTTGAAAGTA-3′		1294–1314 nt
Mut-His^{249}-F	5′-ATGCTGTCA**GAT**GGGACCGAG-3′	Point mutation	736–756 nt
Mut-His ^{249}-R	5′-GATGACCACACAGCAGTCATA-3′		715–735 nt
Mut-Cys^{299}-F	5′-TCCAGGCT**GGT**GGAGGAGGTG-3′	Point mutation	887–907 nt
Mut-Cys^{299}-R	5′-TGAAGAAAAGTTTGGGTTTGCCC-3′		864–886 nt
Mut-Leu^{228}-F	5′-CATGAG**G**TGTCAGCTCTATGT-3′	Point mutation	676–696 nt
Mut-Leu ^{228}-R	5′-TTTGATTTGTCTTTGTTTCAGGTTTG-3′		650–675 nt
P11	5′-ATGGAGGAGCGACACAAGAAGCTTCTG-3′	Tissue distribution and real-time PCR	1–27 nt
P12	5′-CATTCTGAAGCAGCTCCGCCAAACTGTGC-3′		240–268 nt
Actin-F1	5′-GACCTGACAGACTACCTCATG-3′	Actin amplification	550–570 nt
Actin-R1	5′-AGTTGAAGGTGGTCTCGTGGA-3′		821–841 nt

Note: The nucleotide A in start codon ATG was numbered as 1, and the first nucleotide adjacent to the ATG in 5′-UTR was numbered as −1, and so on.

mitochondria in response to the internal apoptotic signal [5,12,13]. After the apoptosome formed, caspase 9 is cleaved at PED^{315}↓ATPF and DQLD^{330}↓AISS to generate the large and small subunits [14–16]. These two subunits then dimerized through a "self-priming" mechanism to form an activated caspase 9, subsequently generating the activated form of downstream caspases 3 and 7. Thereby the apoptotic signal is transmitted to the execution phase [16,17].

Although the structure, regulation and the function of mammalian caspase 9 in apoptosis has been extensively investigated, understanding about caspases 9 in lower vertebrates is limited [18]. In bony fish, only sea bass caspase 9 was characterized [19]. Sea bass caspase 9 was found to be constitutively expressed in most tissues and its mRNA expression and enzyme activity in head kidney was significantly enhanced upon bacterial infection [19]. To fully understand the molecular characteristics and functions of bony fish caspase 9, investigations on caspase 9 from other fish species are needed. In this study, we present the molecular cloning and characterization of caspase 9 gene in the large yellow croaker (*Pseudosciaena crocea*), together with the proteolytic activity of recombinant Lyccasp9 with mutated histidine and cysteine active sites. Tissue distribution and expression modulation of *Lyccasp9* mRNA, as well as enzyme activities of Lyccasp9 in the spleen and kidney upon poly(I:C), a viral mimic or bacterial vaccine stimulation were investigated.

2. Materials and methods

2.1. Fish and challenge experiments

Large yellow croakers (mean weight 200 g) were obtained from mari-culture farm at Lianjiang county, Fuzhou city, China. After 3 days of acclimatizing in aerated seawater tanks, the fish were used for the challenge experiments. Two groups of 30 fish each were injected intramuscularly with poly(I:C) at a dose of 500 μg/200 g fish or inactivated trivalent bacterial vaccine consisting of 1.0×10^8 colony-forming units ml^{-1} of *Vibrio alginolyticus*, *Vibrio parahaemolyticus*, and *Aeromonas hydrophila* each at a dose of 0.5 ml/200 g fish. Inactivated trivalent bacterial vaccine was prepared in our laboratory as previously described [20]. A third group of 30 fish were injected with sterilized phosphate-buffered saline (PBS, pH 7.4) at a dose of 0.5 ml/200 g as a control. The spleens and kidneys were collected from six fish at different time points after stimulation (0, 12, 24, 48 and 72 h) and frozen at −80 °C for RNA extraction.

2.2. Cloning of a partial Lyccasp9 cDNA fragment

Total RNA was extracted from the spleen of large yellow croaker using Trizol® Reagent (Invitrogen) and digested by the RNase-free DNase I (TaKaRa, China) to remove any genomic DNA contamination. First strand cDNA was synthesized with reverse transcription system (TaKaRa) according to the manufacture's protocol. A pair of degenerate primers P1/P2 (Table 1) was designed based on conserved regions of caspase 9 amino acid sequences from other species (human, mouse, rat, dog and sea bass) and used for PCR under following condition: 94 °C for 2 min, then 35 cycles of 40 s at 94 °C, 40 s at 50 °C, 40 s at 72 °C, and final extension at 72 °C for 10 min. The PCR product was cloned into the pMD18-T simple vector (TaKaRa) and sequenced.

2.3. Cloning of full-length cDNA of Lyccasp9

To obtain the full-length cDNA of *Lyccasp9*, 5′ and 3′ RACE-PCR was performed using 5′-Full RACE Kit and 3′-Full RACE Core Set (TaKaRa). Primers for the 5′ and 3′ RACE were designed based on the partial cDNA sequence obtained above. For 5′ RACE, 2–5 μg total RNA was dephosphorylated with calf intestine phosphatase, digested by tobacco acid pyrophosphate (TAP) to remove the 5′ cap structure, and ligated to 5′ RACE Adaptor at 5′ end using T4 RNA ligase. The ligated RNA was transcribed into cDNA with Random 9 mer Primer and used as templates for the subsequent Outer PCR reaction with 5′ RACE Outer Primer/P3 primer. The Inner PCR reaction was performed with 5′ RACE Inner Primer/P4 primer using Outer PCR product as template. The resulting PCR product was cloned into pMD18-T simple vector and sequenced.

For 3′ RACE, 1 μg total RNA was transcribed into cDNA with 3′ RACE Adaptor and used as a template for the subsequent Outer PCR reaction with 3′ RACE Outer Primer/P5 primer. The Inner PCR reaction was performed with 3′ RACE Inner Primer/P6 primer using the Outer PCR product as template. The resulting PCR product was cloned into pMD18-T simple vector and sequenced. All the sequences were assembled and the full-length cDNA of *Lyccasp9*

was obtained. To confirm the integrity of the cDNA sequence, PCR was performed with primer P7 and P8 using the first strand cDNA as a template and the resulted fragment was sequenced.

2.4. Genomic DNA sequence and structure of Lyccasp9

Genomic DNA of large yellow croaker was prepared from muscle according to standard methods [21]. A pair of primers (P7 and P8) was designed based on the *Lyccasp9* cDNA sequence. Fifty nanograms of genomic DNA was used as a template in PCR with an initial denaturation of 5 min at 94 °C, then 35 cycles of 30 s at 94 °C, 30 s at 55 °C and 3 min at 72 °C. The PCR product was cloned into pMD18 simple-T vector. At least two clones were sequenced by M13± sequencing primers.

2.5. Database and sequence analysis

Sequence similarity analysis was performed using BLAST program (http://blast.ncbi.nlm.nih.gov/Blast.cgi). Protein structure was predicted by Prosite Server (http://www.expasy.org/tools/scanprosite/). Multiple sequence alignment was performed using the CLUSTALW program (http://www.ebi.ac.uk/clustaw/). Phylogenetic tree was constructed by Molecular Evolution Genetics Analysis (MEGA) software version 4.0 using the neighbor-joining method [22]. Genomic structure of the *Lyccasp9* gene was analyzed by Genewise online software at http://www.ebi.ac.uk/Tools/Wise2/.

2.6. Expression, purification and proteolytic activity assay of recombinant Lyccasp9 and mutants

Recombinant Lyccasp9 excluding the CARD domain was expressed as an N-terminal 6×His-tagged fusion protein and purified. Briefly, *Lyccasp9* gene fragment encoding residues 120–437 was amplified using the primer set P9 and p10. The PCR product was recovered, digested by EcoRI/HindIII, and then cloned into same enzyme digested pET-His vector (Gene Power Lab, China). The resulted recombinant expression plasmid pET-His-Lyccasp9 was transformed into *Escherichia coli* BL21 (DE3) competent cells. The recombinant Lyccasp9 protein was expressed and purified under denaturing condition by ProBond™ Purification System (Invitrogen). The purified protein was eluted with elution buffer (6 M urea, 0.5 M imidazole, 10 mM Tris–HCl, 50 mM NaCl, pH 4.5) and dialyzed in refolding buffer (containing 4, 2, 1, 0.5, 0.25 or 0 M urea sequentially plus 10 mM Tris–HCl, 50 mM NaCl, pH 7.4) for renaturing. Each dialysis was performed at 4 °C for at least 4 h. Renatured protein was centrifuged at 12,000 rpm for 20 min at 4 °C and the supernatant was transferred to a new tube. The recombinant protein was quantitated by spectrophotometry (ULtrospec2100 pro, Pharmacia Biotech). Recombinant large yellow croaker β-actin (rLycactin) was expressed in the same system, and purified as a control.

To obtain mutated rLyccasp9, three pairs of primers creating site-directed mutagenesis (Primers Mut-His^{249}-F and Mut-His^{249}-R caused mutation of the His^{249} to aspartic acid. Primers Mut-Cys^{299}-F and Mut-Cys^{299}-R caused mutation of the Cys^{299} to glycine. Primers Mut-Leu^{228}-F and Mut-Leu^{228}-R caused mutation of the Leu^{228} to valine, Table 1) were designed and PCR amplification was performed with the MutanBEST Kit (TaKaRa). The recombinant expression plasmid pET-His-Lyccasp9 was used as template. The resulting expression plasmid containing the mutation was sequenced to confirm the site-directed mutagenesis. Recombinant protein expression, purification and renaturing were performed as above.

The proteolytic activity of all proteins was detected using the Caspase 9 Activity Assay Kit (Beyotime, China) according to the manufacturer's manual. Briefly, the purified protein was adjusted to 2 μg/μl. Then 80 μl reaction buffer, 10 μl of protein solution and 10 μl 2 mM substrate (Ac-LEHD-*p*NA) were mixed sequentially and incubated at 37 °C for 2 h. The cleavage and release of *p*NA was measured by monitoring the absorbance at 405 nm using spectrophotometer. The activity of rLyccasp9 was defined as hydrolyzing activity of Ac-LEHD-*p*NA, and expressed as times of caspase 9 activity of negative control rLycactin.

2.7. Tissue expression profile analysis of Lyccasp9 by RT-PCR

Various tissues including spleen, kidney, blood, liver, heart, gills, intestine, and muscle were collected from at least three healthy fish. Total RNA was isolated, treated with RNase-free DNase I and transcribed into first strand cDNA using Oligo dT-Adpator primer (TaKaRa). To determine the tissue expression profile of *Lyccasp9*, RT-PCR was performed with a gene-specific primer set of P11 and P12 (Table 1). β-*Actin* was amplified as an internal control to determine the concentration of each template with the primer set of Actin-F1 and Actin-R1 (Table 1). PCR conditions were: 3 min at 94 °C, then 30 cycles of 30 s at 94 °C, 40 s at 55 °C and 40 s extension at 72 °C, followed by 10 min at 72 °C.

2.8. Expression analysis of Lyccasp9 by real-time PCR

Total RNA was extracted from spleen and kidney tissues of three fish sampled at 0, 12, 24, 48 and 72 h after stimulation with poly(I:C) or inactivated trivalent bacterial vaccine, respectively. Tissues from fish injected with sterilized PBS buffer as control were sampled at same time. The first strand cDNA was synthesized from 1 μg of each total RNA and used as template for real-time PCR with primer set of P11 and P12. Real-time PCR was performed on ABI 7500 Real-time PCR system (Applied Biosystems) using SYBR® *Premix ExTaq*™ (TaKaRa). Cycling conditions were 95 °C for 3 min, followed by 40 cycles of 95 °C for 20 s, 56 °C for 20 s, and 72 °C for 1 min. The fluorescence output for each cycle was measured upon the completion of the entire run. Cycle threshold values were calculated by the SDS software algorithms (Applied Biosystems) and converted into equivalent target amount (ETA) using the statistical standard curve established using the calibrator. The expression levels of *Lyccasp9* were expressed relative to that of β-*actin* by calculating the ratio of ETA *Lyccasp9* and ETA β-*actin* as previously described [23].

2.9. Proteolytic activity analysis of Lyccasp9 in spleen and kidney upon stimulation with poly(I:C) or inactivated trivalent bacterial vaccine

Spleen or kidney tissues were sampled at 0, 12, 24, 48 and 72 h after stimulation with poly(I:C), bacterial vaccine or sterilized PBS buffer, respectively. Then 3–10 mg tissues were homogenized on ice in 100 μl lysis buffer (25 mM HEPES, 5 mM $MgCl_2$, 5 mM EDTA, 5 mM dithiothreitol, 2 mM phenylmethylsulfonyl fluoride, pH 7.5) and incubated on ice for 5 min. The lysate was centrifugated at 18,000 × *g*, 4 °C for 15 min and supernatant was transferred to a new microtube. The protein concentration of the supernatant was determined and adjusted to 2 μg/μl with lysate buffer. The proteolytic activity of Lyccasp9 was then detected by Caspase 9 Activity Assay Kit (Beyotime, China) as described by manufacturer's manual.

2.10. Statistical analysis

All proteolytic activity analysis and real-time PCR were repeated three times, and all data were analyzed using SASS software and expressed as mean ± S.E.M. Two-tailed Student *t*-test

was used to determine the significant difference of gene expression levels or proteolytic activity between the experiment group and the control group. A P value <0.05 was considered to be statistically significant.

3. Results

3.1. Lyccasp9 cDNA and genomic structure

The determined *Lyccasp9* cDNA (EU878545) is 2595 nucleotides (nt) long and includes a 5′-untranslated region (UTR) of 214 nt and a 3′-UTR of 1067 nt. One mRNA instability motif (ATTTA) and a typical polyadenylation signal (AATAAA) are located 792 nt and 26 nt upstream of the poly(A) tail, respectively (data not shown). The 1314 nt open reading frame (ORF) of *Lyccasp9* encodes a protein of 437-aa, which exhibits a typical caspase 9 domain architecture containing a putative N-terminal CARD domain (residues 1–90), a caspase family p20 domain (residues 171–303) and p10 domain (residues 348–435). Caspase family signature histidine active-site H^{236}SQYDCCVVIMLSHG^{250}, cysteine active-site K^{290}PKLFFI-QACGG^{301} and caspase 9 characteristic pentapeptide active-site QACGG are located in the p20 domain (Fig. 1A). Multiple sequence alignment shows that human caspase 9 active-site residues Arg^{180}, His^{237}, Cys^{287}, Trp^{354} and Arg^{355}, as well as Asp^{315} and Asp^{330} where the cleavage to generate p20 domain and p10 domain occurs, are all conserved in large yellow croaker caspase 9 (Fig. 1A).

Multiple sequence alignment and phylogenetic tree showed fish and human caspase 9 were highly evolutionarily conserved. The catalytic subunits of fish and human caspase 9 exhibited high sequence similarity ranging from 55 to 59%, while the prodomains are more divergent with the sequence similarities ranging from 33 to 40%. Genetically, Lyccasp9 is closest to European sea bass caspase 9 (Fig. 1B).

The genomic DNA sequence of *Lyccasp9* (EU878547) is 3836 bp, containing 10 exons and 9 introns (Fig. 2). The nine introns are 402, 91, 76, 99, 94, 103, 114, 149 and 113 nt in length, respectively. All introns conform to the typical intron-splicing motif (GT/AG rule). Genomic analysis showed that *Lyccasp9* has a similar intron/exon organization to sea bass and human caspase 9, although intron 3 that is present in caspase 9 of large yellow croaker and sea bass is absent in human caspase 9 (Fig. 2).

3.2. Expression, purification and proteolytic activity assay of recombinant Lyccasp9 and mutants

The *Lyccasp9* gene fragment excluding the CARD domain was cloned into the pET-His vector and expressed as 6×His-tagged protein. After IPTG induction, total cellular protein of induced pET-His/BL21 and pET-His-Lyccasp9/BL21 was analyzed by SDS-PAGE. A 38 kDa band corresponding to the recombinant Lyccasp9 could be visualized by Commassie blue staining (Fig. 3B). The rLyccasp9 was then purified using 6×His-tag under denaturing conditions and renatured. The mutated rLyccasp9-Mut-His^{249}-D, rLyccasp9-Mut-Cys^{299}-G and rLyccasp9-Mut-Leu^{228}-V were also produced, purified and renatured (Fig. 3B).

The proteolytic activity assay showed that the hydrolyzing activity of rLyccasp9 was 56.21 times that of rLycactin. With His^{249} mutated to aspartic acid or Cys^{299} mutated to glycine, the enzyme activities of rLyccasp9-Mut-His^{249}-D and rLyccasp9-Mut-Cys^{299}-G were only 4.88 and 3.08 times that of rLycactin, corresponding to 8.68 and 5.46%, of rLyccasp9, respectively. There were significant differences in the hydrolyzing activity between these two mutant proteins and rLyccasp9 (P value <0.01). However, the mutation on Leu^{228} did not cause the change in hydrolyzing activity, since the enzyme activity of rLyccasp9-Mut-Leu^{228}-V was 53.63 times that of rLycactin, almost equivalent to that of rLyccasp9 (Fig. 3C). These results indicated both histidine and cystein active sites are essential for maintaining the large yellow croaker caspase 9 activities and the cysteine active site is more important than the histidine active site.

3.3. Tissue expression profile of Lyccasp9

To investigate the tissue expression profile of *Lyccasp9*, RT-PCR was performed to analyze its transcription in various tissues. As shown in Fig. 4, the *Lyccasp9* mRNA was constitutively expressed in all tissues examined, and at the highest levels in heart and blood, and at the lowest levels in intestine and muscle, indicating that *Lyccasp9* was broadly expressed in various tissues although at different levels (Fig. 4).

3.4. Expression modulation of Lyccasp9 in spleen and kidney upon stimulation with poly(I:C) or inactivated trivalent bacterial vaccine

To further understand the modulation of *Lyccasp9* expression upon stimulation with poly(I:C) or bacterial vaccine, real-time PCR analysis was employed to detect the mRNA levels of *Lyccasp9* in spleen and kidney during 72 h of induction. The results showed that the mRNA levels of *Lyccasp9* in both spleen and kidney were quickly up-regulated by either poly(I:C) or bacterial vaccine, reaching peak levels at 48 h and then decreasing by 72 h post-induction. After poly(I:C) stimulation, *Lyccasp9* transcript was increased up to 15.0- and 12.9-fold in spleen and kidney, respectively. Upon inoculation with bacterial vaccine, *Lyccasp9* transcript reached 13.2- and 11.4-fold in spleen and kidney, respectively (Fig. 5).

3.5. Proteolytic activity analysis of Lyccasp9 in spleen and kidney upon stimulation with poly(I:C) or inactivated trivalent bacterial vaccine

The proteolytic activities of Lyccasp9 in spleen and kidney upon poly(I:C) or bacterial vaccine stimulation were detected by Ac-LEHD-*p*NA hydrolyzing assays, respectively. After bacterial vaccine stimulation, the proteolytic activity of Lyccasp9 in spleen and kidney were increased from 12 h post-stimulation, and reached the peak at 48 h (about 5.68- and 3.61-fold increase, respectively). After poly(I:C) stimulation, enzyme activity of Lyccasp9 in spleen reached the peak at 48 h (3.34-fold increase), and then decreased slightly at 72 h. In kidney, the Lyccasp9 activity reached the peak at 12 h (2.91-fold increase) and then decreased (Fig. 6).

4. Discussion

BLAST and Prosite analysis clearly indicate that the protein encoded by this cDNA sequence is a homologue of caspase 9. It contains a typical caspase 9 domain architecture including a putative CARD domain followed by caspase family p20 and p10 domain (large and small subunit). To further analyze the fish caspase 9 homologue, we mined the cDNA and protein sequence of caspase 9 homologue of European sea bass, *Dicentrarchus labrax* and rainbow trout, *Oncorhynchus mykiss*, from the NCBI GenBank, as well as the deduced caspase 9 protein sequence of pufferfish, *Takifugu rubripes*, green spotted puffer, *Tetraodon nigroviridis*, stickleblacks, *Gasterosteus aculeatus*, zebrafish, *Danio rerio*, and medaka, *Oryzias latipe* from ENSEMBL database. The high similarity shown by multiple alignments between fish and human caspase 9 amino acid sequences, especially in the catalytic subunits, indicates the caspase 9 is evolutionarily conserved (Fig. 1A). In humans, after the apoptosome forms, the cleaving activity of caspase 9 proform increases up to 2000-fold [16]. The first cleavage

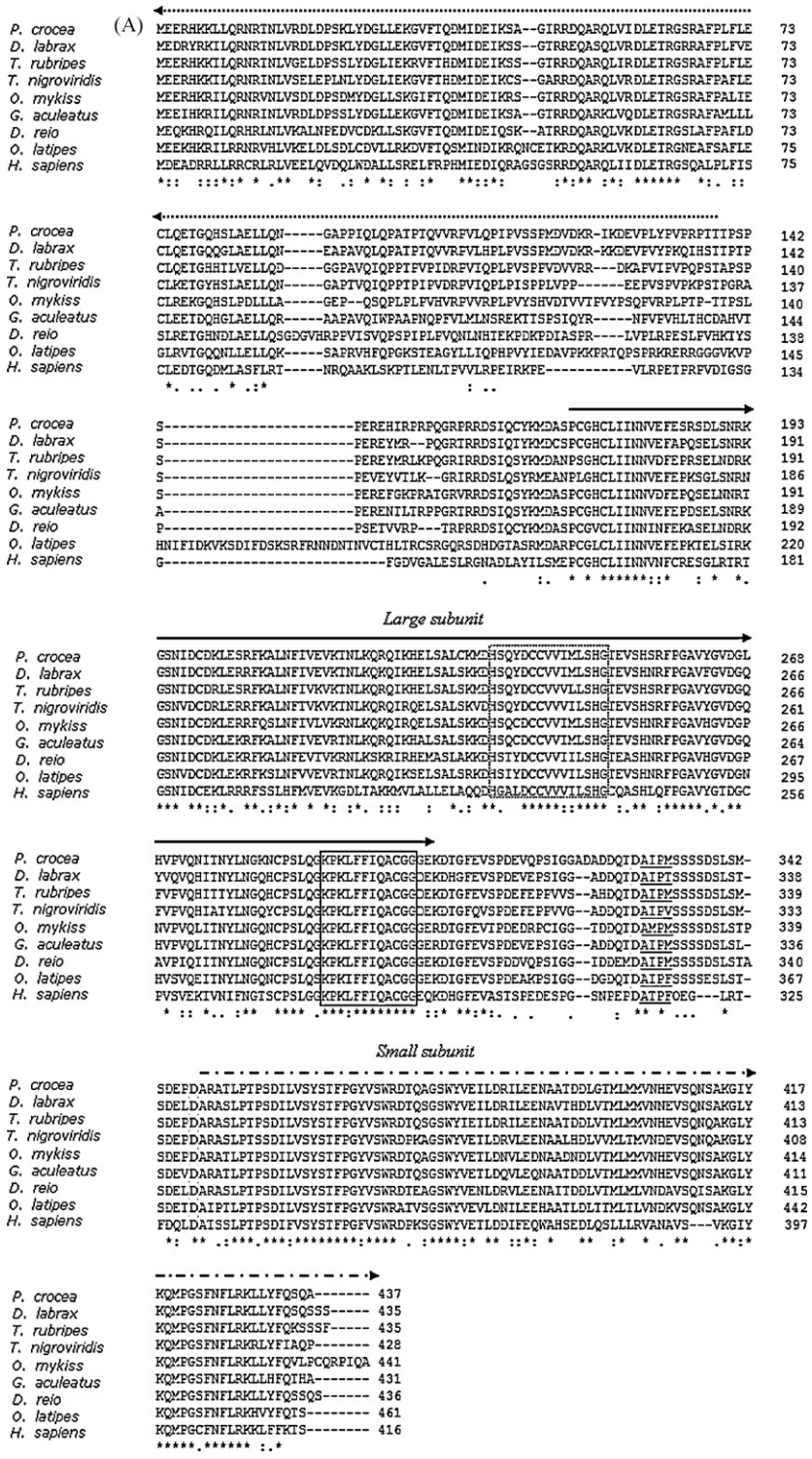

Fig. 1. (A) Multiple alignment of Lyccasp9, other fish caspase 9 homologues and human caspase 9 amino acid sequences. The caspase family histidine and cysteine active sites were boxed in a discontinuous or continuous line, respectively. The putative cleavage site at aspartic acid residues, which separates the large subunit (→) from the small subunit (–·–▶) was shaded in gray. The prodomains are indicated by dashed line with an arrow head (◀·····). The A-X-P-X motifs are underlined. The numbers indicate the amino acid positions and dashes indicate gaps introduced to optimize similarity between sequences. Asterisks and ": and ." denote residues identical in all sequences and chemical similarity between amino acids, respectively. (B) Phylogenetic tree based on the genetic distances of the deduced amino acid sequences of caspase 9 between bony fish and vertebrates. The tree was constructed by MEGA software version 4.0 (Tamura et al. [22]) using neighbor-joining methods. Numbers on nodes represent frequency with which this node is recovered per 100 bootstrap replications in a total of 1000. The GenBank accession numbers of caspase 9 amino acid sequences used here are as follows: *Pseudosciaena crocea* EU878545; *Oncorhynchus mykiss*, AAY88917; *Dicentrarchus labrax*, ABC70999; *Homo sapiens* AAH02452.1; *Xenopus laevis*, BAA94750.1; *Rattus norvegicus*, NP_113820.1; Other sequences are mined from the Ensemble Genome Site (www.ensembl.org) and the protein sequence ID are: *Takifugu rubripes* ENSTRUP00000045371; *Tetraodon nigroviridis* ENSTNIP00000013855; *Gasterosteus aculeatus* ENSGACP00000007379; *Danio rerio*, ENSDARP00000047019; *Oryzias latipe*, ENSORLP00000003208.

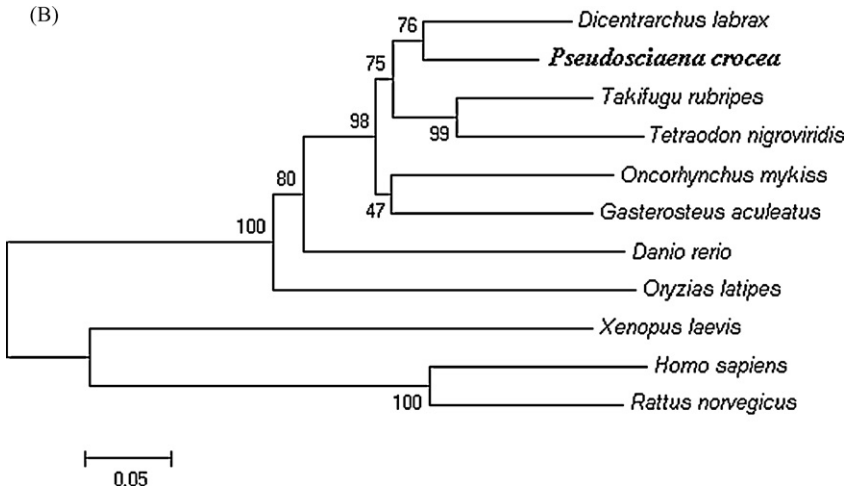

Fig. 1. (*Continued*).

of caspase 9 happens at Asp^{315}. This cleavage not only generates the large subunit, but also produces an N-terminal ATPF (Ala-Thr-Pro-Phe) motif, which can interact with XIAP (inhibitor of apoptosis protein) to inhibit the caspase-processing activity of the apoptosome. ATPF motif shares significantly homology with the N-terminal IAP-binding motif (AVPI) of Smac (second mitochondrial activator of caspases), which is also released from the mitochondria and has a higher binding affinity to the ATPF motif. Smac then competitively displaces XIAP from caspase 9 and allow caspase 9 to process procaspase-3, which in turn cleaves caspase 9 at Asp^{330}, removing the ATPF motif from the small subunit, completely disrupting the inhibition of XIAP on caspase 9 [24,25]. The large subunit and small subunit then dimerize through a "self-priming" mechanism to form an activated caspase 9, subsequently generating the active form of downstream caspases 3 and 7, to transmit the apoptotic signal to the execution phase [16,17]. Homology comparison showed that the Asp^{315} and Asp^{330} are conserved in all fish caspase 9 homologues, and all fish caspase 9 have an A-X-P-X four-peptide motif similar to the ATPF motif of human caspase 9 (Fig. 1A), indicating that fish caspase 9 may experience the same cleavage as its human counterpart. Moreover, all the fish caspase 9 contain a CARD domain of about 90-aa, histidine and cysteine active sites of caspase family, and conserved residues important for human caspase 9 activity, such as Arg^{180}, His^{237}, Cys^{287}, Trp^{354} and Arg^{355} [17]. In addition, all fish caspase 9 have an A-X-P-X four-peptide motif similar to the ATPF motif of human caspase 9 (Fig. 1A). Amino acid sequence homology and structure similarity suggest a functional conservation between bony fish and mammalian caspase 9.

In humans, when the active-site QACGG of caspase 9 was mutated into QASGG or QAAGG, the mutant could still bind to Apaf-1 and form the apoptosome, but could not activate the caspase 3, thus apoptosis was blocked [26]. To investigate whether the caspase family active sites are also important in maintaining the activity of Lyccasp9, we performed site-directed mutagenesis and the recombinant mutants were expressed in *E. coli*. Proteolytic activity assay showed that the rLyccasp9-Mut-His^{249}-D has about 8.68% activity of the wild-type rLyccasp9, while the rLyccasp9-Mut-Cys^{299}-G possesses only 5.46% activity of the wild-type rLyccasp9, indicating that both histidine and cysteine active sites in Lyccasp9 are essential for maintaining the proteolytic activity as those in human caspase 9.

Tissue expression profile analysis showed that *Lyccasp9* was constitutively expressed in all tissues examined with heart and blood containing the highest levels and intestine and muscle containing the lowest levels (Fig. 5). This expression pattern is partly similar to that of sea bass, human and rat caspase 9 genes, where the highest expression levels were observed in heart and liver [15,19,27]. In this study, *Lyccasp9* was expressed at a relatively high level in kidney and spleen, however, in sea bass, humans and rat, the expression levels of caspase 9 in spleen and kidney are low [15,19,27].

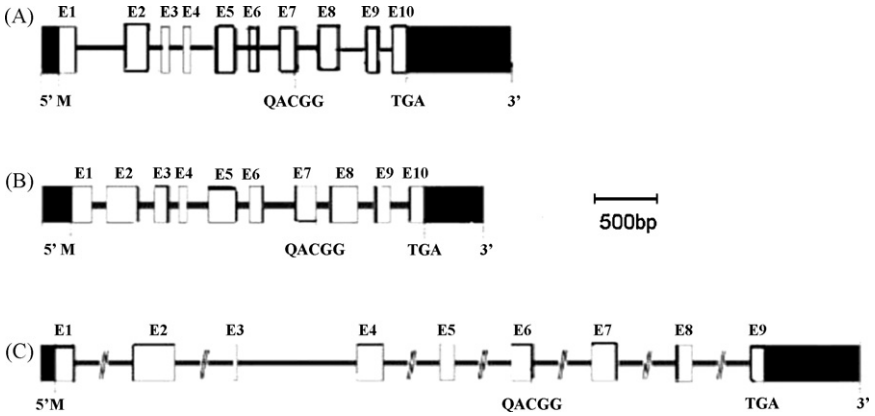

Fig. 2. Schematic representation of genomic organization of caspase 9 from large yellow croaker (A, EU878547), European sea bass (B, DQ345776) and human (C). The genome sequence of human caspase 9 was obtained from Ensemble Genome Site with transcription ID ENST00000333868. The exons are indicated by white boxes and introns are indicated by solid line. The 5′ and 3′ untranslated regions are represented by black boxes, respectively.

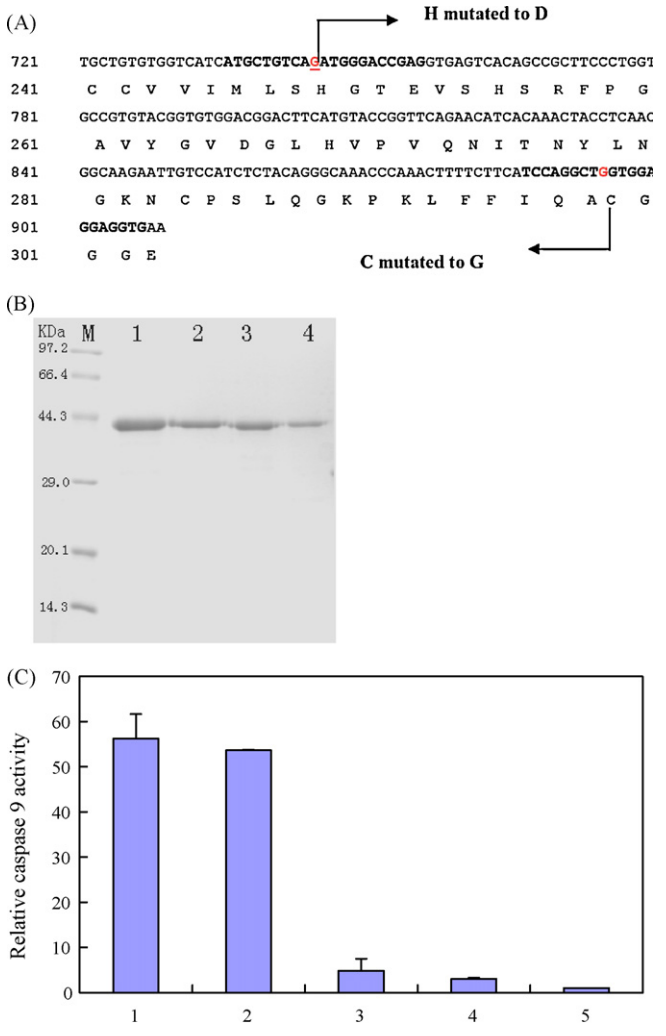

Fig. 3. Expression, purification and proteolytic activity assay of recombinant Lyccasp9 and mutants. (A) Schematic of site-directed mutagenesis. (B) SDS-PAGE analysis of purified and renatured rLyccasp9 as well as mutants. M: protein molecular weight standards; lane 1: renatured rLyccasp9; lane 2: renatured rLyccasp9-Mut-Leu^{228}-V; lane 3: renatured rLyccasp9-Mut-Cys^{299}-G; lane 4: renatured rLyccasp9-Mut-His^{249}-D. (C) Proteolytic activity assay. The proteolytic activity of all proteins was detected by Caspase 9 Activity Assay Kit (Beyotime, China) as described by manufacturer's manual. Briefly, the purified and renatured protein was adjusted to 2 μg/μl. Then 80 μl reaction buffer, 10 μl of protein solution and 10 μl 2 mM substrate (Ac-LEHD-*p*NA) were mixed sequentially and incubated at 37 °C for 2 h. The cleavage and release of *p*NA was measured by monitoring the absorbance at 405 nm using spectrophotometer. The activity of rLyccasp9 was defined as hydrolyzing activity of Ac-LEHD-*p*NA and expressed as folds of the activity of negative control rLycactin. Column 1, wild-type rLyccasp9; column 2, rLyccasp9-Mut-Leu^{228}-V; column 3, rLyccasp9-Mut-His^{249}-D; column 4, rLyccasp9-Mut-Cys^{299}-G; column 5, rLycactin as negative control.

To understand the expression modulation of *Lyccasp9* upon poly(I:C) or bacterial vaccine stimulation, the transcriptional levels of *Lyccasp9* in spleen and kidney tissues were analyzed at different time points post-induction. The results showed *Lyccasp9* transcript

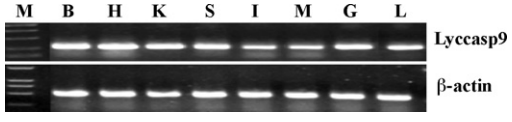

Fig. 4. Tissue expression profile of *Lyccasp9*. Total RNA was extracted and transcribed into cDNA from blood, heart, spleen, intestine, muscle, gills and liver of three healthy fish. RT-PCR was used to detect the expression levels of *Lyccasp9* mRNA. β-*Actin* was amplified as an internal control. M: DL-2000 DNA marker; B – blood; H – heart; K – kidney; S – spleen; I – intestine; M – muscle; G – gill; L – liver.

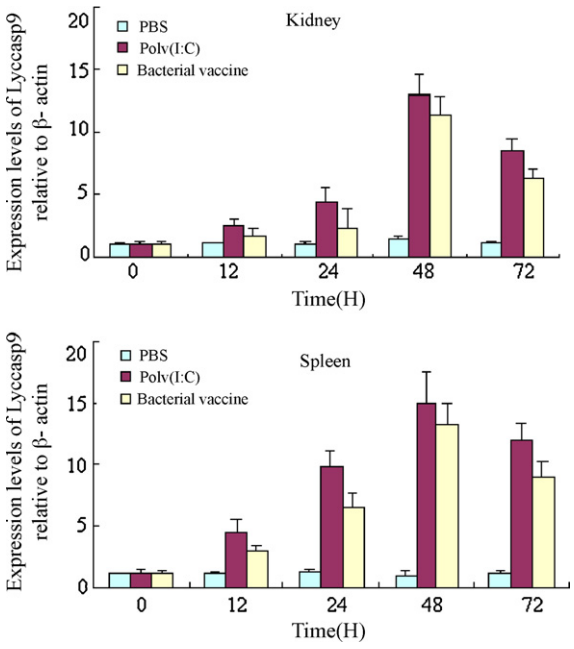

Fig. 5. Expression modulation of *Lyccasp9* in spleen and kidney upon stimulation with poly(I:C) or inactivated trivalent bacterial vaccine by real-time PCR. Total RNA was extracted from spleens and kidneys sampled at different time points post-stimulation, transcribed into cDNA and used for real-time PCR detection. Expression of β-*actin* was used as an internal control for real-time PCR. Each experiment was performed in triplicate. Deviation bars represent the standard errors of the mean.

in both tissues was increased at 12 h, reaching the peak at 48 h and then decreasing by 72 h post-induction (Fig. 5). Similar results were observed in sea bass, in which the caspase 9 mRNA expression in head kidney was increased and reached the peak at 12 h post-infection, and then declined to a basal level at 24 h [19]. One possible reason for the difference in the time that Lyccasp9 and sea bass caspase 9 mRNA reached the peak levels is that the stimulant used in our study was inactivated bacterial vaccine whereas Reis and colleagues used live pathogenic bacteria as a stimulant in their study [19]. In mammals, the increase in activities of the initiator caspase 9 indicates that the intrinsic apoptotic pathway is activated [5,28]. Here the enzyme activities of both Lyccasp9 were increased upon stimulation with poly(I:C) or bacterial vaccine (Fig. 6), suggesting that the intrinsic apoptotic

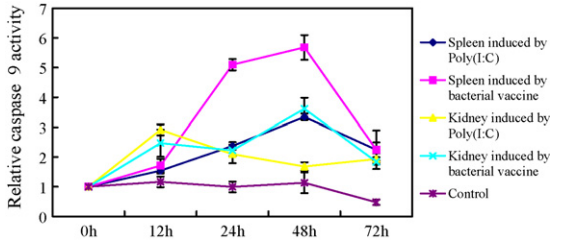

Fig. 6. Proteolytic activity analysis of Lyccasp9 in spleen and kidney upon stimulation. Spleen or kidney tissues were sampled at 0, 12, 24, 48 and 72 h after stimulation with poly(I:C) or inactivated trivalent bacterial vaccine. Then 3–10 mg tissues were homogenized on ice in 100 μl lysis buffer (25 mM HEPES, 5 mM $MgCl_2$, 5 mM EDTA, 5 mM dithiothreitol, 2 mM phenylmethylsulfonyl fluoride, pH 7.5) and incubated on ice for 5 min. The lysate was centrifugated at 18,000 × *g*, 4 °C for 15 min and supernatant was transferred to a new microtube. Protein concentration of the supernatant was determined and adjusted to 2 μg/μl with lysate buffer. The enzymatic activity of Lyccasp9 was detected by Caspase 9 Activity Assay Kit (Beyotime, China), and calculated as hydrolyzing activity of Ac-LEHD-*p*NA. For each group, caspase activity of sample at 0 h was defined as 1 and caspase activities of samples at other time point were compared with it.

pathway may be involved in the immune response induced by poly(I:C) or bacterial vaccine in large yellow croaker.

Acknowledgements

The work was supported by grants from Nation '863' Project under contract Nos. 2006AA100306, 2006AA10A405 and 2007AA091406, and National Natural Science Foundation of China (30871925). The authors thank Miss Pamela Willan in the school of Life Sciences, University of Manchester, for her help in English language editing.

References

[1] Kerr JF, Wyllie AH, Currie AR. Apoptosis: a basic biological phenomenon with wide-ranging implications in tissue kinetics. Br J Cancer 1972;26(4):239–57.
[2] Wyllie AH, Kerr JF, Currie AR. Cell death: the significance of apoptosis. Int Rev Cytol 1980;68:251–306.
[3] Earnshaw WC, Martins LM, Kaufmann SH. Mammalian caspases: structure, activation, substrates, and functions during apoptosis. Annu Rev Biochem 1999;68:383–424.
[4] Thornberry NA, Lazebnik Y. Caspases: enemies within. Science 1998;281(5381): 1312–6.
[5] Hakem R, Hakem A, Duncan GS, Henderson JT, Woo M, Soengas MS, et al. Differential requirement for caspase 9 in apoptotic pathways in vivo. Cell 1998;94(3):339–52.
[6] Lawen A. Apoptosis—an introduction. Bioessay 2003;25:888–96.
[7] Salvesen GS, Dixit VM. Caspases: intracellular signaling by proteolysis. Cell 1997;91(4):443–6.
[8] Hofmann K, Bucher P, Tschopp J. The CARD doma: a new apoptotic signalling motif. Trends Biochem Sci 1997;22(5):155–6.
[9] Reed JC. Mechanisms of apoptosis. Am J Pathol 2000;157(5):1415–30.
[10] Marsden VS, Strasser A. Control of apoptosis in the immune system: Bcl-2, BH3-only proteins and more. Annu Rev Immunol 2003;21:71–105.
[11] Strasser A, O'Connor L, Dixit VM. Apoptosis signaling. Annu Rev Biochem 2000;69:217–45.
[12] Saleh A, Srinivasula SM, Acharya S, Fishel R, Alnemri ES. Cytochrome c and dATP-mediated oligomerization of Apaf-1 is a prerequisite for procaspase-9 activation. J Biol Chem 1999;274(25):17941–5.
[13] Zou H, Li Y, Liu X, Wang X. An APAF-1.cytochrome c multimeric complex is a functional apoptosome that activates procaspase-9. J Biol Chem 1999; 274(17):11549–56.
[14] Green DR, Reed JC. Mitochondria and apoptosis. Science 1998;281(5381): 1309–12.
[15] Srinivasula SM, Fernandes-Alnemri T, Zangrilli J, Robertson N, Armstrong RC, Wang L, et al. The Ced-3/interleukin 1beta converting enzyme-like homolog Mch6 and the lamin-cleaving enzyme Mch2alpha are substrates for the apoptotic mediator CPP32. J Biol Chem 1996;271(43):27099–106.
[16] Twiddy D, Cain K. Caspase-9 cleavage, do you need it? Biochem J 2007;e1–2.
[17] Renatus M, Stennicke HR, Scott FL, Liddington RC, Salvesen GS. Dimer formation drives the activation of the cell death protease caspase 9. Proc Natl Acad Sci USA 2001;98(25):14250–5.
[18] Krumschnabel G, Podrabsky JE. Fish as model systems for the study of vertebrate apoptosis. Apoptosis 2009;14(1):1–21.
[19] Reis MI, do Vale A, Pinto C, Nascimento DS, Costa-Ramos C, Silva DS, et al. First molecular cloning and characterisation of caspase-9 gene in fish and its involvement in a gram negative septicaemia. Mol Immunol 2007;44(7): 1754–64.
[20] Zheng W, Tian C, Chen X. Molecular characterization of goose-type lysozyme homologue of large yellow croaker and its involvement in immune response induced by trivalent bacterial vaccine as an acute-phase protein. Immunol Lett 2007;113(2):107–16.
[21] Sambrook J, Fritsch EF, Maniatis T, editors. Molecular cloning: a laboratory manual. 2nd ed., New York: Cold Harbor Laboratory Press; 1989.
[22] Tamura K, Dudley J, Nei M, Kumar S. MEGA4: molecular evolutionary genetics analysis (MEGA) software version 4.0. Mol Biol Evol 2007;24(8):1596–9.
[23] Liu G, Zhang J, Chen X. Molecular and functional characterization of a CD59 analogue from large yellow croaker *Pseudosciana crocea*. Mol Immunol 2007;44(15):3661–71.
[24] Shiozaki EN, Chai J, Rigotti DJ, Riedl SJ, Li P, Srinivasula SM, et al. Mechanism of XIAP-mediated inhibition of caspase-9. Mol Cell 2003;11(2):519–27.
[25] Srinivasula SM, Hegde R, Saleh A, Datta P, Shiozaki E, Chai J, et al. A conserved XIAP-interaction motif in caspase-9 and Smac/DIABLO regulates caspase activity and apoptosis. Nature 2001;410(6824):112–6.
[26] Li P, Nijhawan D, Budihardjo I, Srinivasula SM, Ahmad M, Alnemri ES, et al. Cytochrome c and dATP-dependent formation of Apaf-1/caspase-9 complex initiates an apoptotic protease cascade. Cell 1997;91(4):479–89.
[27] Angelastro JM, Moon NY, Liu DX, Yang AS, Greene LA, Franke TF. Characterization of a novel isoform of caspase-9 that inhibits apoptosis. J Biol Chem 2001;276(15):12190–200.
[28] Boatright KM, Salvesen GS. Mechanisms of caspase activation. Curr Opin Cell Biol 2003;15(6):725–31.